RSC Advances

PAPER

View Article Online
View Journal | View Issue

Cite this: *RSC Adv.*, 2015, **5**, 75311

Using water to modify the localization of clay in immiscible polymer blends

Fang Du,[a] Mohamed Yousfi,[a] Pascale Lipnik,[b] Michel Sclavons[b] and Jérémie Soulestin*[a]

Bio-based polyamide 11 (PA11) and water-soluble polyethylene oxide (PEO) (80/20 wt/wt) were used to prepare an immiscible polymer blend. Ternary systems containing 1 wt% hydrophilic clay (organomodified or native clay) were elaborated using extrusion with and without injection of water. The cryoscopic effect on PA11 and PEO observed by high pressure differential scanning calorimetry indicated that they were both miscible with water under conditions of water-assisted extrusion. Transmission electron microscopy revealed a selective localization of both types of clay in the matrix (PA11). However, with water-assisted extrusion a part of the organomodified clay platelets was localized into the dispersed phase (PEO). Under rheological tests, the unmodified clay exhibited a different effect compared with the organomodified clay on the modulus and viscosity of the blend. The van Gurp–Palmen plot indicated that clay potentially decreased the interfacial tension between PA11 and PEO, while the weighted relaxation spectra confirmed that water improved the dispersion state of the clay and limited the polymer degradation. Thermogravimetric analyses showed that the presence of clay and water improved the thermal stability of PA11/PEO blends. Our work is the first one which has realized water-assisted extrusion of a clay-filled ternary blend.

Received 29th June 2015
Accepted 27th August 2015

DOI: 10.1039/c5ra12594d

www.rsc.org/advances

Introduction

Blending of two polymers becomes an efficient way for developing new materials with combined properties, which are not available in pristine polymers. However most polymers are immiscible and exhibit a phase-separated morphology with very poor mechanical properties, thus limiting their potential applications. A classic solution to this problem is using physical or reactive compatibilization methods to decrease the polymer–polymer interfacial tension and to obtain thinner morphology. Block and graft copolymers are one of the most used compatibilizing agents to improve the compatibility between immiscible polymers.[1,2] Another advantage of these copolymers is covalent coupling between polymers phases that induces an increase of interfacial adhesion.

Recently, a number of studies have revealed that nanoparticles as carbon nanotubes, silica and clays can also be used to compatibilize polymer blends and reinforce their structural properties.[3,4] In the case of clays, it could have different effects on the blend, such as decrease of the interfacial tension, and modification of coalescence behavior.[5,6] The localization of the clay particles in polymer blends is assumed to play an important role in the morphology and the mechanical properties of blends. When clay is localized in the continuous matrix phase generally a reduced size of the minor phase is observed due to a decrease in the interfacial tension between the two polymers. In addition, the barrier effect of the clay at the interface and the increase of the melt viscosity of the matrix could also help reduce the dispersed phase size. However, it has already been proved in many cases when the nanofiller is localized in the dispersed phase, its average size could be eventually increased.[7,8] Moreover, the nature of blend components, the dispersion degree of clay and the interaction between each phase could also influence the ultimate properties.

In order to improve the compatibility between the polymer and clay, natural montmorillonite clay is generally modified with organophilic alkylammoniums,[9] leading to a larger interlayer spacing and lower clay surface energy.[10] The organomodified clay thus facilitates the separation and dispersion of the clay platelets into the polymer matrix. Nevertheless, alkylammonium surfactants are not thermally stable. It decomposes at higher extrusion temperatures and thus leads to the collapse of the silicate layers.[11] Furthermore, the organoclays have been reported to have catalytic effect on the degradation of polymers[12–15] and plasticizing effect[16] due to surfactant. In this context, water-assisted extrusion was firstly reported[17] to obtain exfoliated PA6/clay nanocomposites using unmodified clay

[a]*Department of Polymer and Composite Technology & Mechanical Engineering, Mines Douai, 941 rue Charles Bourseul, CS 10838, F-59508 Douai Cedex, France. E-mail: fang.du@mines-douai.fr; mohamed.yousfi@mines-douai.fr; jeremie.soulestin@mines-douai.fr; Fax: +33 3 27 71 29 81; Tel: +33 3 27 71 21 80*

[b]*Bio- and Soft Matter, Institute of Condensed Matter and Nanosciences, Université Catholique de Louvain, Croix du Sud 1, Box 4, B-1348 Louvain-la-Neuve, Belgium. E-mail: pascale.lipnik@uclouvain.be; michel.sclavons@uclouvain.be*

instead of the expensive clay organomodification. In fact, water exhibits multiple effects during the melt-extrusion process on both clay and polymers. On one hand, it has been reported that the injection of water facilitates the diffusion of polymer chains between the clay platelets by increasing the polarity and fluidity of polymer and the interlayer spacing of clays.[18,19] On the other hand, the catalytic degradation induced by clay and the plasticizing effect of surfactant on the polymer matrix could be removed by injection of water through the steam flushing of volatile extrusion-degraded surfactant throughout the degassing apertures.[20] This has also been confirmed by detailed odor and volatile organic compound (VOC) emission analysis.[21]

In this study, bio-based polyamide 11 (PA11) and water soluble poly ethylene oxide (PEO)[22] were chosen as a polymer pair. First of all, they were assumed to be immiscible polymers according to their different polarities and surface tension. Secondly, PA11/clay and PEO/clay composites have already been investigated and showed both very good polymer–clay interactions with a good exfoliation level. PA11 as other polyamides presents good affinity with clay due to its highly polar amide functions.[23] The polar and hydrophilic PEO has also revealed strong interactions with clays as it adsorbs fast on clay surface[24] by forming hydrogen bonds between the ether oxygen and the silanols on the silicate surface.[25] In addition, the hydrophobic siloxanes of clay surface also present high affinity with the alkyl chains of PEO.[26] As a result, the localization of clay in the binary immiscible blend and the properties of corresponding blends formed would be very interesting to look at. Furthermore, considering the potential interactions between clay and these polymers, the effect of water injection during extrusion on the localization of clay is of high interest. Indeed, a better dispersion can be expected in the case of water-assisted extrusion.[18] On the other hand, since PEO is a water-soluble polymer and clays generally present great affinity with water too, it is highly probable that clay would migrate between the two polarity-different phases with the aid of water.

An unmodified clay and two organomodified clays of different surface polarity were used to see their respective localization and their effect on blend morphology and rheological properties. A systematic comparison between the unfilled and clay filled blends was highlighted. In addition, a comparison between the PA11/PEO/clay blends prepared with and without injection of water during processing reveals an interesting effect of water on the ultimate properties of the compounds.

Experimental

Materials

PA11 (BECNO TL) was supplied by Arkema (France) in pellet form. Its melt flow rate is 30 g/10 min (235 °C, 2.16 kg). PEO (Polyox WSR N-750) was supplied by Dow Chemical Company (Netherlands) in powder form. Its melt flow rate is 3–4 g/10 min (190 °C, 2.16 kg). According to the material data sheet, the PEO contains about 3% fumed silica (generic) and 1% calcium as mixed salts. Three kinds of clay were used: an unmodified montmorillonite Cloisite Na^+, referred to as C-Na^+; two types of organomodified montmorillonite Cloisite 15A (referred to as C15A) and Cloisite 30B (referred to as C30B). C30B is more hydrophilic than C15A due to the hydroxyl functions on the alkylammonium modifier. All clays were supplied by Southern Clay Products (USA). Water was used directly from lab tap, (referred to as "w" in the following tables and figures).

Sample preparation

PA11 was dried before extrusion during 24 hours in a vacuum oven at 80 °C. All the other materials were used as received. The unfilled and clay-based PA11/PEO blend were prepared using a twin-screw co-rotating extruder Coperion ZSK 26 MC (Coperion, Germany) with a screw diameter of 25 mm and a length to diameter ratio of 40. Mixing was carried out at a screw speed of 150 rpm and a temperature of 220 °C was set up for the 10 heating zones of the extruder. PA11, PEO (or PEO dry mixed with clay) were introduced into the extruder simultaneously. All blends prepared were constituted of 80 wt% PA11 and 20 wt% PEO. In case of addition of clay, it was introduced simultaneously with PA11 and PEO and its content in the blend was maintained at 1 wt% in order to avoid a significant modification of the viscosity ratio. The extruder is equipped with a water injection pump and two degassing vents. In case of extrusion assisted by water, the pressure of water was maintained at about 20 bars and water was injected in the compression zone just after the convoying zone. Its throughput was adjusted to be equal to PEO throughput (∼20 wt%). Extruded strands were cooled into a water bath and then pelletized. The resulting pellets were then injection-molded using an injection molding machine Babyplast model 610P (Cronoplast SL, Spain). The temperature was set up at 220 °C in all heating zones. Dogbone specimens (standard ISO 527-2) were molded for tensile test, discs (diameter of 35 mm and thickness of 2 mm) for rheology.

Sample characterization

The miscibility of PA11 and water at high pressure and high temperature was investigated using a high pressure differential scanning calorimeter HPDSC 827e (Mettler Toledo, Switzerland). A pressure controlling valve PC-5866 series (Brooks Instrument, USA) was connected to the measuring chamber. The pressure was maintained at 20 bars during the heating and cooling cycles to simulate the extrusion conditions. PA11 pellets were firstly freeze-ground with a Pulverisette 14 Rotor Mill (Fritsch/Idar-Oberstein, Germany) in order to obtain a homogeneous contact between polymer and water. PA11 or PEO powder and water were mixed at a weight ratio of ∼2/1, with a total sample weight of ∼13 mg. First heating was conducted from 30 to 160 °C with 10 minutes of stabilization (homogenization of contact polymer–water), then from 160 to 220 °C with 1 minute of stabilization, which was followed by cooling from 220 to 30 °C with 1 minute of stabilization and a second heating from 30 to 220 °C. The heating and cooling rate was maintained at 10°C min^{-1}.

The dispersion of the clay platelets in the blend was observed using a transmission electron microscope (TEM). TEM images were carried out on the extruded pellets. Ultrathin sections were

prepared using a microtome Leica EM FC6 at the temperature of −80 °C for knife, sample, and chamber. The knife used for cutting was a diatome cryowet at 35°. Ultrathin sections of 150 nm thick were then collected on a 200 mesh carbon grid. Observations were carried out using a TEM LEO 922 (Carl Zeiss, Germany) at the acceleration tension of 120 kV. All images were obtained by a CCD camera.

A scanning electron microscope SEM S4300 SE/N (Hitachi, Japan) was utilized to observe the cryofractured surfaces of injection-molded specimens. The specimens were cryofractured in liquid nitrogen, and then etched in water during 1 hour in order to remove the PEO phase and highlight the contrast between the different phases. The specimen surfaces were coated with gold during 45 seconds at 2.4 kV before SEM observations. The average diameter of the dispersed phase was calculated using ImageJ software by measuring the average Feret diameter[27] of 200 droplets.

Rheological analyses were performed using a rotational rheometer HAAKE MARS III (Thermo Scientific, Germany). Injection-molded disks obtained from extruded pellets were used for these tests after being dried in a vacuum oven prior to experiment at 80 °C during 24 hours. All measurements were performed at 220 °C in nitrogen atmosphere, in parallel-plate geometry with 35 mm diameter plates and a 1.8 mm gap size. Linear domains of different samples were identified from strain sweeps and a common strain of 1% was chosen for all samples. Frequency sweeps were carried out between 0.1 and 100 rad s^{-1}. The storage modulus (G'), loss modulus (G''), and complex viscosity ($|\eta^*|$) were measured as function of the angular frequency. Rheological results of pure PA11 were obtained in the same preparation way as other blends, while those of pure PEO were obtained by direct injection in a Haake Minijet II (Thermo Scientific, Germany) without extrusion due to the very high viscosity of PEO.[28] To investigate the effects of nanoclay and water-assisted extrusion process on the relaxation behaviors of PA11/PEO samples, the relaxation spectra $H(\lambda)$ of neat polymers and blends were calculated. $H(\lambda)$ were obtained from the storage modulus *vs.* angular frequency data using the standard non-linear regularization NLREG method integrated in the commercial software package RheoWin (Thermo-Scientific, Germany).[29]

Thermogravimetric analysis of different blends was conducted by using a TGA/DSC 1 (Mettler Toledo, Switzerland) under air flow from 30 to 700 °C with a heating rate of 10°C min^{-1}. Thermal stability was evaluated through the temperature at 5% weight loss ($T_{5\ wt\%}$). $T_{5\ wt\%}$ is generally considered as the critical decomposition temperature since the weight loss before this temperature is attributed to water evaporation.

Results and discussion

High pressure differential scanning calorimetry (HPDSC)

As water-assisted extrusion was used during preparation of some of our blends, the miscibility of PA11 and PEO with water is of high interest. Besides the PEO which is soluble in water at atmospheric pressure, polyamides have also been reported to be fully soluble in water at high temperature under pressure.[18,30,31] HPDSC results of both polymers with and without water at 1 bar and 20 bars are presented in Fig. 1. At 20 bars, water boiling point is 215 °C (ref. 32) and thus does not appear in the temperature range of the HPDSC thermograms. As expected, the melting temperatures of both polymers are not significantly affected by the pressure increase from 1 bar to 20 bars. These observations are in agreement with what have been reported by other authors, where an increase in pressure of 100 bars just brings a shift in melting temperature of less than 2 °C.[33,34] On the other hand, in the presence of water the melting temperatures of both polymers are largely decreased at 20 bars, showing cryoscopic effect. In the case of PEO, its melting peak has shifted down by ~12 °C, while that of PA11 has decreased by ~28 °C in the presence of water due to the single phase

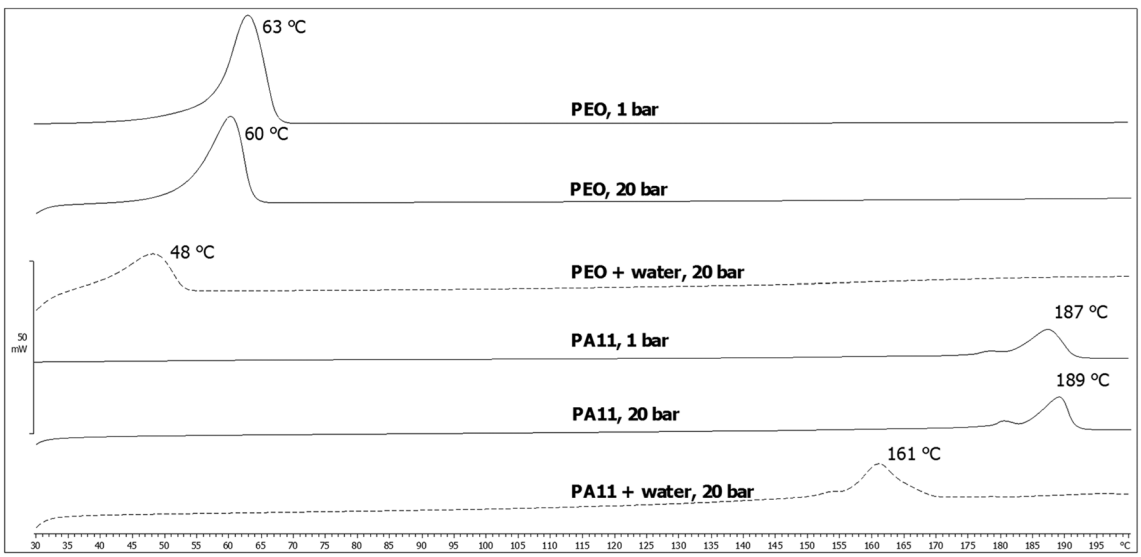

Fig. 1 HPDSC thermograms of the second heating for PA11 and PEO with and without water at 1 bar and 20 bars.

constituted of water and PA11. H-bonds can be formed between water and the amide groups, hence the solvatation of PA11 by water.[35] The cryoscopic effect of water onto polyamide melting occurs once the pressure is above the water vapor pressure, and remains the same whatever the pressure.[30,31,36] PA11 shows more significant cryoscopic effect than PEO due to the its more efficient water adsorption mechanism, where three molecules of water are bound on two neighboring amide groups in saturated conditions.[37] The theoretical ratio of water/PA11 in saturated conditions is calculated using the equation:

$$\frac{n_{PA11}}{n_{H_2O}} = \frac{2}{3} \rightarrow \frac{m_{PA11}}{m_{H_2O}} = \frac{2}{3}\frac{183}{18} = \frac{183}{27}$$

$$\frac{m_{H_2O}}{m_{syst}} = \left(1 + \frac{m_{PA11}}{m_{H_2O}}\right)^{-1} = 0.13,$$

where n the number of molecule and m the corresponding weight. A minimum concentration of 13 wt% of water is required to obtain complete solvatation of PA11 (the amount of water used in HPDSC tests and extrusion 20 wt% was in excess). The shift in melting temperature of PA11 is lower than that of PA6 reported because of its lower concentration in amide group compared to PA6. Considering the discussions above, it can be confirmed that water and PA11 or PEO could form a single molten phase in the extrusion conditions, with higher polarity and lower viscosity than that of PA11 or PEO, which according to the mechanism proposed by Fedullo *et al.* facilitates the polymer ability to diffuse into the clay, and the desorption of water molecule.[18]

Transmission electron microscopy (TEM)

TEM has been used to evaluate the dispersion of clay and its localization in the blends depending on extrusion conditions. Particularly, it aims at highlighting the effect of water-assisted extrusion. Fig. 2 shows TEM micrographs for PA11/PEO blends containing 1 wt% of the different clays. The bright area corresponds to the PEO phase while the gray area is the PA11 phase. In all images, the black round particles and their aggregates are silica originally present in the PEO (~3 wt% in order to help increase the flowability according to the material data sheet). Only the black long platelets in the images correspond to the exfoliated nanoclay or/and the agglomerated stacks. It can be seen that irrespective to the clay added, the nanoclay platelets are selectively localized in PA11 phase only. The comparative observation of the three different blends tends to show that the exfoliation of clay seems to be higher in the blend containing C30B. It seems that clays have more affinity with the continuous PA11 phase because of the hydrogen bonds formed between polar amide functions and clay surface. However, PEO should also present high affinity with clay because of the hydrogen bonds between the ether oxygen and the silanols,[25] and the hydrophobic interactions between alkyl segments along the PEO backbone and siloxanes.[26] In fact, Derho *et al.* observed that clay is always agglomerated in PEO, regardless of its loading, in PLA/PEO/clay ternary systems.[38] In our case, the selective localization of clay platelets in PA11 could be explained by the fact that nanoparticles tend to be localized in the phase with lower viscosity.[39–41] The viscosity of PEO revealed by the melt flow rate in the material data sheet is much higher than that of PA11.

With the water-assisted extrusion, clays are still mainly localized in the PA11 matrix with an even better dispersion degree than in the corresponding blend without water, as shown in Fig. 3. As a result, water-assisted extrusion improves the dispersion degree of clay.[18] The C30B blend in presence of water exhibits still the most homogeneous dispersion. Meanwhile, some platelets of clay have been observed in PEO and at the interface PA11/PEO of the blends with C15A and C30B in the presence of water. The partial localization in PEO could be explained by the fact that water/PEO miscibility improves the mutual interdiffusion of PEO and clays by increasing PEO polarity and decreasing its viscosity.[18] Furthermore, the injection of water brings a lubricating effect of the process medium which reduces the high viscosity of the PEO phase and thus facilitates the migration of clay.

On the other hand, none of the clay platelets can be observed in PEO for the composite C-Na^+. Despite the fact that the unmodified hydrophilic C-Na^+ should have high affinity with water and with the hydrophilic PEO phase compared with the organomodified ones and that the interlayer Na^+ cations could be complexed by polyethers to form crown-ether like cryptates due to strong Na^+–ether coordination,[42] clay layers are still only present in the PA11 phase. A reasonable explanation for this is that PA11 shows, according to the molecular simulation, better thermodynamical interactions with unmodified clay due to a

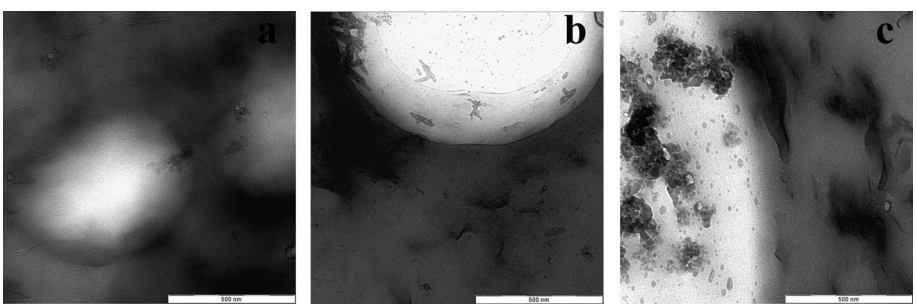

Fig. 2 TEM micrographs of PA11/PEO blend containing (a) C15A, (b) C30B and (c) C-Na^+.

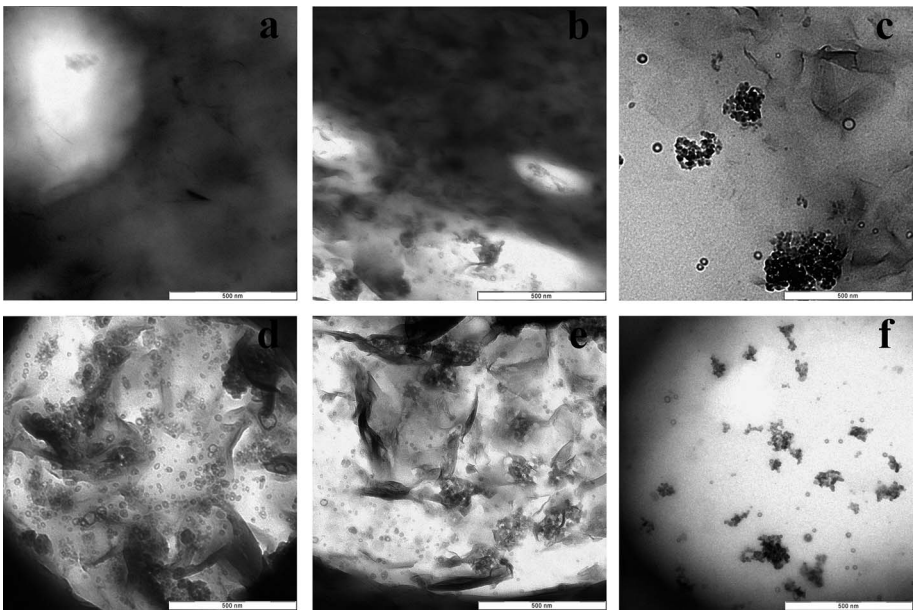

Fig. 3 TEM micrographs of PA11/PEO blend prepared by water-assisted extrusion, high magnification at the interface in (a) C15A, (b) C30B and (c) C-Na^+, inside the PEO (d) C15A, (e) C30B and (f) C-Na^+.

much higher binding energy as compared to the organo-modified clay[43,44] and the effect of water is not enough to break it. Finally, independently of the type of clay, silica particles are always in the PEO phase, confirming the flocculant effect of PEO on this kind of particles.[24,45] No migration of silica particles is observed from PEO to PA11 with the injection of water. Therefore it can be reasonably considered that the presence of silica particles does not influence the selective localization of clay in the blends.

Scanning electron microscopy (SEM)

It is nowadays well admitted that nanofillers like clay could affect the morphology of polymer blends. In order to evaluate the effect of water-assisted extrusion and clay on morphology, all blends were observed using SEM. Fig. 4 show micrographs of water-etched cryofractured surfaces of the different blends. The holes correspond to the position of the water-extracted PEO phase. The micrographs confirm that the two polymers are immiscible and the blend presents a droplet morphology. Table 1 summarizes the average diameter of PEO droplet in the unfilled blend and the corresponding clay-based blends and Fig. 6 represents the droplet size distribution. FWHM (full width at half maximum) was also measured in order to evaluate the polydispersity of diameter values (Table 1). The polydispersity of the droplet size is not modified by the presence of clay. In all cases, the average droplet size of PEO is slightly decreased with the presence of clay. Firstly, the decrease in droplet sizes may be caused by the selective localization of clay in the PA11 phase and the increase of PA11 viscosity, which leads to a reduced viscosity ratio. Furthermore, in immiscible polymer blends, the shape and size of droplets under flow (in extruder) are determined by both the shearing forces and the pressure distribution around the droplets. The former is connected with the viscosity and the latter with the elastic properties of the melt components. The elasticity of the melt is characterized by the so-called first normal stress differences. When the difference in the first normal stress differences of the droplet phase and the matrix is positive, the elasticity acts under shear conditions as an additional interfacial tension. In the opposite case, when the elasticity of the droplet phase is smaller than that of the matrix, the interfacial tension is reduced under shear according to the following equation:[46]

$$\Gamma_{\text{in the presence of flow}} = \Gamma_{\text{in the absence of flow}} + \frac{D_0}{12}(N_{1,\text{d}} - N_{1,\text{m}}),$$

where Γ is the interfacial tension, D_0 the initial diameter of droplets and $N_{1,\text{d}}$ and $N_{1,\text{m}}$ the first normal stress differences of the dispersed phase and matrix respectively. The preferential localization of clay in the matrix (PA11) will induce an increase of matrix elasticity. As a result, the interfacial tension is decreased and the deformation and breakup of droplets become easier which could explain the decrease in the mean diameter of PEO phase in the presence of clay.

The decrease of interfacial tension can be supported by using the equation of Serpe:[47]

$$D \approx \frac{\left[\frac{4\Gamma_{\text{PEO/PA11}}}{\dot{\gamma}\eta_{\text{blend}}}\left(\frac{\eta_{\text{PEO}}}{\eta_{\text{blend}}}\right)^{0.84}\right]}{1-(4\Phi_{\text{PEO}}\Phi_{\text{PA11}})^{0.8}},$$

where D is the average diameter of the dispersed phase, Γ the interfacial tension, $\dot{\gamma}$ the shear rate, η the viscosities of the dispersed phase and the blend, and Φ the volume fraction of the two phases. Later rheological analyses show that the presence of clay decreases the viscosity of the blend, while the

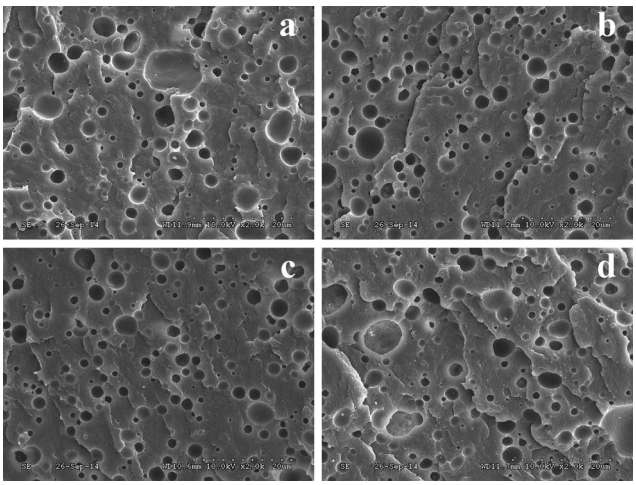

Fig. 4 SEM micrographs of (a) unfilled PA11/PEO, and blends containing (b) C15A, (c) C30B and (d) C-Na^+.

Table 1 Average and FWHM (full width at half maximum) diameter of droplet in the unfilled and clay-based blends without and with water injection

Sample	D_N (μm)	FWHM (μm)
PA11/PEO 80/20	2.8	2.4
PA11/PEO 80/20 w	3.4	2.2
1% C15A	2.2	2.0
1% C15A w	3.6	3.0
1% C30B	1.7	2.4
1% C30B w	2.2	2.2
1% C-Na^+	1.8	2.2
1% C-Na^+ w	2.6	2.4

viscosity of PEO could not be modified since there is no clay particle. Therefore, only the decrease of the interfacial tension Γ could result in the reduced size of droplet between PA11 and PEO.

Fig. 5 shows the SEM micrographs of different blends processed with the injection of water during extrusion. The droplet size in all blends is increased slightly in the presence of water and the PEO phase becomes irregular in shape. The compatibilizing effect of clays on immiscible PA11/PEO disappears probably due to the clay particles localized into PEO phase instead of PA11 which leads to an increased viscosity ratio. The increase in the melt viscosity of the dispersed phase and decrease in that of the matrix, leads to higher viscosity ratio and elasticity ratio, which could favor the increase of droplet size.[48] In fact, the localization of a few clay platelets in PEO instead of PA11 could have significant effect on the dispersed phase since the local concentration of clay in PEO could become higher than that in PA11 due to the low content of dispersed phase (20 wt%). More clay platelets observed at the interface of PA11/PEO could also hinder the rounding promoted by the interfacial tension, which results in the irregular shape formed.[5,6]

Rheological behavior

In order to investigate the influence of clay and its localization on the relaxation of the dispersed phase, rheological tests have been carried out on different blends without and with the injection of water. The storage modulus and the complex viscosity as a function of the frequency are presented in Fig. 7. As it can be seen from Fig. 7a and b, PEO is much more elastic and viscous than PA11. At high frequencies, the viscosity of PEO is 8 to 10 times higher than that of PA11. At low frequencies, PA11 shows a Newtonian plateau behavior, while PEO exhibits a shear thinning behavior over all frequencies. Fig. 7c and d showed that in our case regardless of the type of clay added, both modulus and viscosity are decreased over the frequency range of 0.1–100 rad s^{-1}, especially in the case of organo-modified clays. These behaviors are in contrast with those observed by most authors where there is an increase of both the modulus and viscosity with the addition of clay generally at higher clay content and especially in case of exfoliated platelets. The low amount of clay used, their low degree of exfoliation as observed by TEM and therefore the lack of their interaction (lower surface area) with the PA11 matrix are not good enough to improve the viscoelastic properties. Fornes *et al.* have also pointed out a reduced viscosity of PA6/clay compared with the pure PA6 because of matrix molecular mass degradation.[49,50]

In Fig. 7c, the storage modulus of clay-based blends is reduced without any solid-like behavior at low frequencies and shows the same frequency dependence or liquid-like behavior as the unfilled blend. A solid-like behavior at low frequencies which is commonly observed in the nanocomposites mostly refers to clay contents over 3–5 wt% to perform a percolated three-dimensional filler network structure.[51,52]

In Fig. 7d two distinct regions of viscosity are noted: at low frequencies (below 0.5 rad s^{-1}), a Newtonian region with plateau behavior, while at higher frequencies, the viscosity decreases with the frequency and shows a power-law region with shear thinning behavior indicating the existence of yield

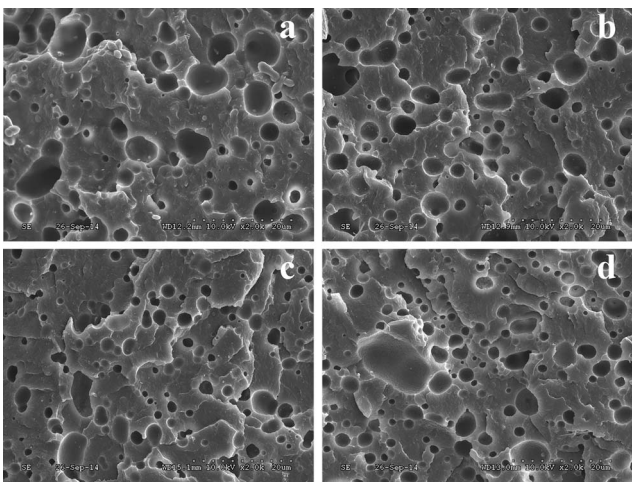

Fig. 5 SEM micrographs of (a) unfilled PA11/PEO, and blends containing (b) C15A, (c) C30B and (d) C-Na^+, prepared by water-assisted extrusion.

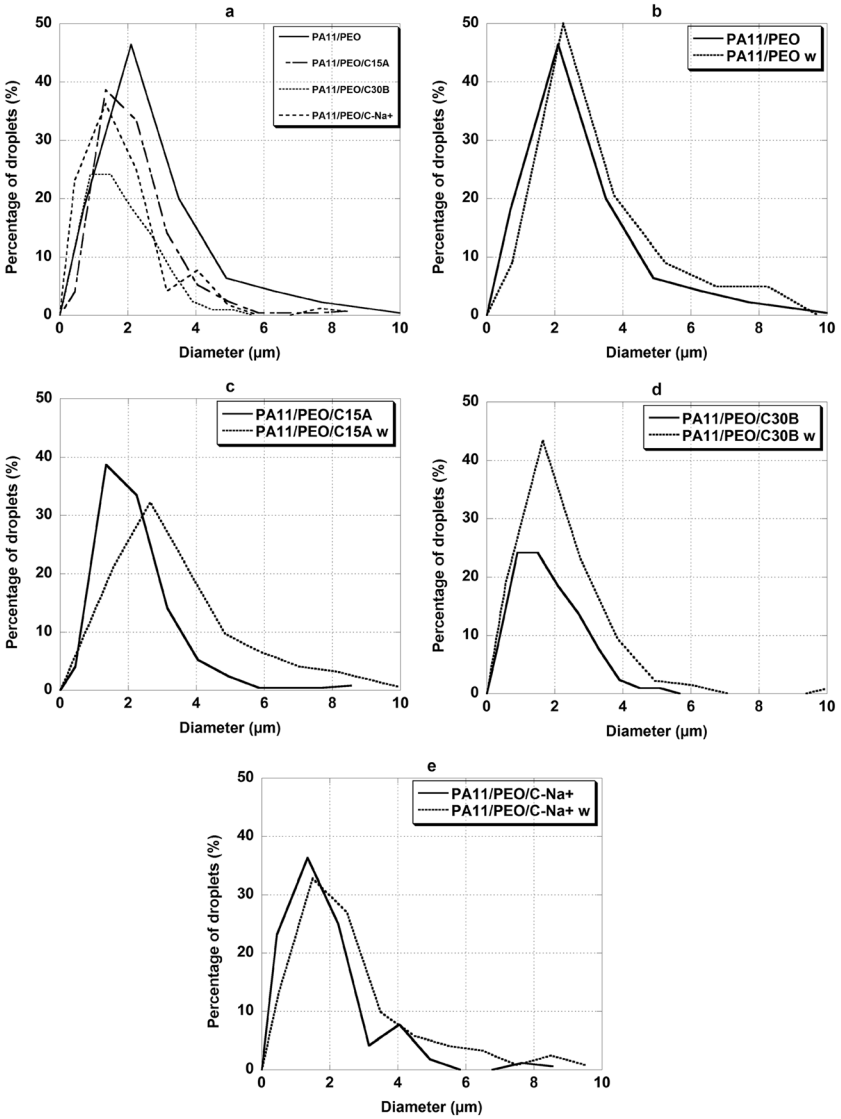

Fig. 6 Distribution of PEO droplet size in unfilled and clay filled PA11/PEO blends, (a) without and (b–e) with injection of water.

stress. The span of the Newtonian plateau remains almost the same regardless of the type of clay. Although the viscosities of all clay-based blends are reduced, there seems to be slightly less rapid shear thinning flow at higher frequencies compared to that of the unfilled blend. Among the three clays used, C-Na^+ blend exhibits a slightly different behavior in the high frequency region where its viscosity remains almost the same as that of the unfilled blend. C-Na^+ leads to no plasticizing effect on the viscosity of the blend already observed in PA nanocomposites[16] due to the absence of surfactant.

The storage modulus and the viscosity as a function of the frequency presented in Fig. 8 and 9 when water is injected during extrusion process. Both the storage modulus and the viscosity of the unfilled PA11/PEO blend are reduced when adding water, due to probable hydrolysis of the PEO (ether functions). On the other hand, polyamides are generally more stable in the presence of water.[53] In contrast, those of the clay-based blends are increased with addition of water potentially due to improved dispersion of clay platelets which is in good agreement with the better clay dispersion in the two phases observed by TEM. Moreover, clay-based blends suffer less plasticization caused by free and degraded surfactant molecules due to the steam flushing,[16] and less catalyzed degradation due to surfactant stabilization onto clay surface by water lubricating effect[20] which lead to the increase in the modulus and viscosity. C-Na^+ blend exhibits a weak increase of both the storage modulus and viscosity when adding water probably due to a less uniform dispersion and a lack of clay particles in PEO.

Relaxation behaviour

Fig. 10 shows the van Gurp–Palmen plot (vGP) (the phase angle 'δ', *versus* the absolute complex modulus '$|G^*|$'), of the studied samples. The van Gurp–Palmen plot (vGP) is originally devoted to the characterization of polydispersity of linear polymers, and to the detection of the changes in the topology (long-chain

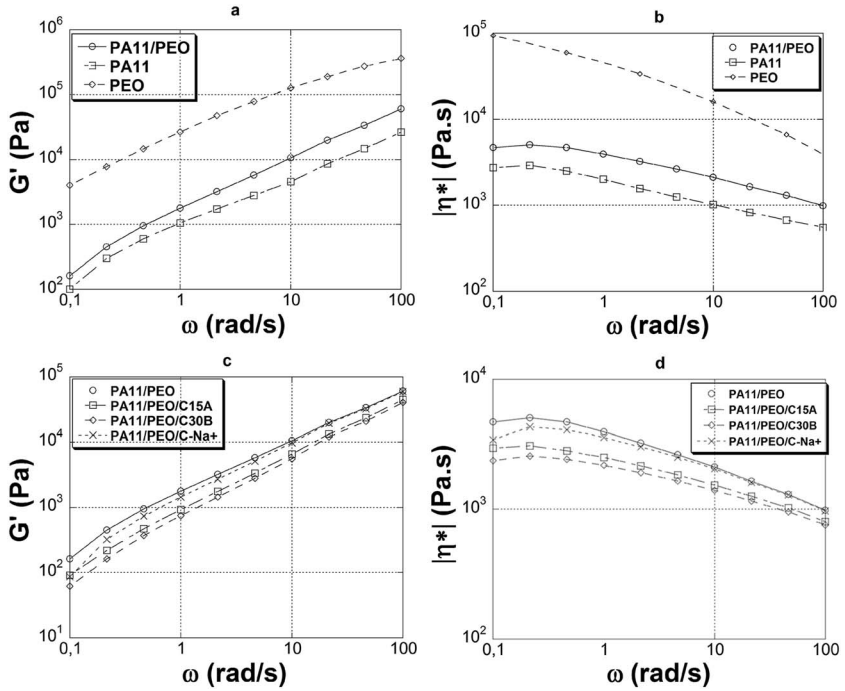

Fig. 7 Storage modulus G' and complex viscosity $|\eta^*|$ as a function of the frequency ω for (a) and (b) neat polymers and blend, (c) and (d) unfilled and clay-filled blend.

branching) in polymers according to the theory of Trinkle and Friedrich.[54] This plot was later used to probe the rheological percolation in polymer nanocomposites,[55,56] to identify the relaxation species in a complex polymeric system, to obtain information on the morphology and the degree of compatibility in the case of immiscible polymer blends.[57,58]

In the case of PA11/PEO blends, the vGP plot contains a minima (tail of long relaxation times) corresponding to the major component (PA11) and a maxima reflecting the high frequency shape relaxation of the dispersed phase (PEO). This shape of (vGP) plot is characteristic of the matrix/droplet morphology.[58]

The clay-based blends display higher values of the phase angle in comparison with the pure PA11/PEO blends, reflecting a general decrease of the elasticity.[57] In the case of PA11/PEO/C-Na^+, this effect is less pronounced due to its lower dispersion state. The (vGP) plot shifted towards the lower complex modulus (long relaxation times) with the addition of the clay, particularly in the presence of C15A and C30B. The position of the maximum in the (vGP) spectrum is known to be correlated to the ratio of the interfacial tension to the dispersed phase radius (α/R).[57] An α/R decrease, indicates that the shape relaxation of droplets occurs at low frequency (long relaxation times). Since the size of nodules in the clay filled blends is reduced as compared to that in the unfilled blend, the interfacial tension is thus lowered after the addition of the organoclay, and less pronounced in the case of raw C-Na^+ blend.

Fig. 11 shows the van Gurp–Palmen (vGP) plot of samples extruded with and without water injection. With the addition of water in pure PA11/PEO blends, the (vGP) plot is slightly shifted towards the lower $|G^*|$, indicating a slight decrease in α/R, which is coherent with the increase of droplet size observed by SEM. In contrary, the addition of water during melt extrusion of clay-based blends leads to a decrease of the phase angle 'δ' and a slight shift of the (vGP) spectra to the higher complex modulus which means an elasticity of the blends increase principally due to the enhancement in the dispersion state of the filler. These observations are consistent with ones of the TEM and the previous rheological interpretations on the storage modulus and the complex viscosity.

In order to investigate the effect of clay and water on the relaxation behaviours of PA11/PEO blends, the weighted relaxation spectra $\lambda H(\lambda)$ from Honerkamp and Weese (HW) plots can be used to reflect the chain relaxation time distribution for neat polymers[59,60] and immiscible polymer blends.[61] The relaxation spectra $H(\lambda)$ of viscoelastic polymers in frequency domain can be estimated from the measured storage modulus G' using the standard nonlinear regularization NLREG method integrated in the commercial software package RheoWin (ThermoScientific, Germany)[29] which is a numerical procedures in C++ based on the regularization method proposed by Honerkamp and Weese:[60]

$$G'(\omega) = \int_{-\infty}^{+\infty} H(\lambda) \frac{\omega^2\lambda^2}{1+\omega^2\lambda^2} \mathrm{d}(\ln \lambda),$$

where ω is the angular frequency and λ the relaxation time. Fig. 12 shows the HW relaxation plot of PA11, PEO and PA11/PEO blend. The characteristic relaxation time corresponding to PA11 is $\approx$3.6 s. The PEO exhibits a broader relaxation spectrum with lower characteristic relaxation time. The maxima in

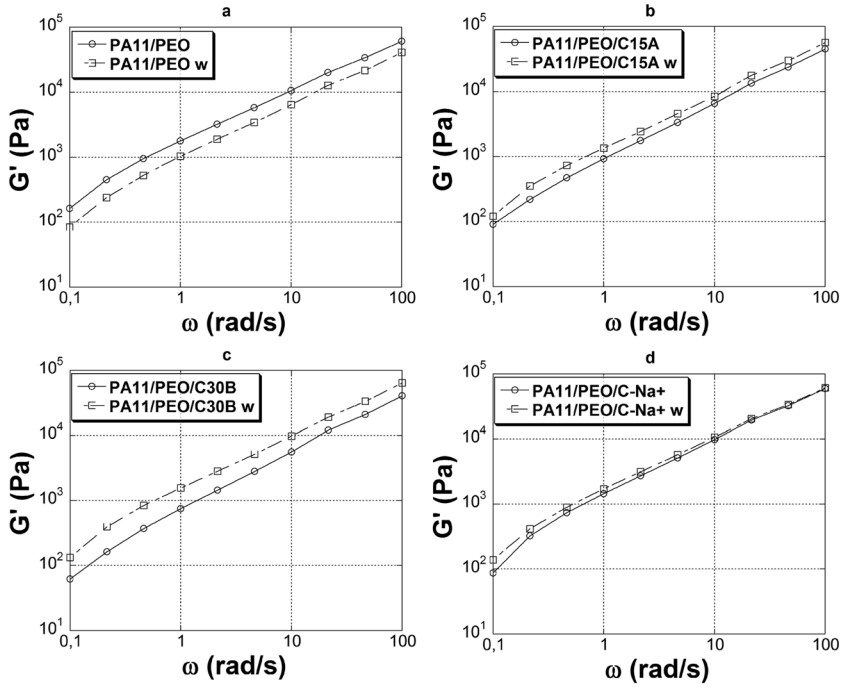

Fig. 8 Comparison of water-assisted to dry-processed storage modulus G' as a function of the frequency ω of (a) the unfilled PA11/PEO, and blends containing (b) C15A, (c) C30B and (d) C-Na^+.

the large peak correspond to ≈0.2 s. In the case of PA11/PEO blend, two characteristic peaks corresponding respectively to the dispersed PEO phase and the matrix are distinctly observed. The PA11 relaxation peak is not modified, while that of PEO is shifted towards the lower relaxation times ($\lambda \approx 0.06$ s) probably due to the effect of processing conditions (the pure PEO was injected without extrusion because of high viscosity).

Fig. 13 illustrates a comparison between the relaxation spectra of unfilled PA11/PEO and clay-based blends. For the PA11/PEO/C-Na^+ sample, the HW plot has a single large peak

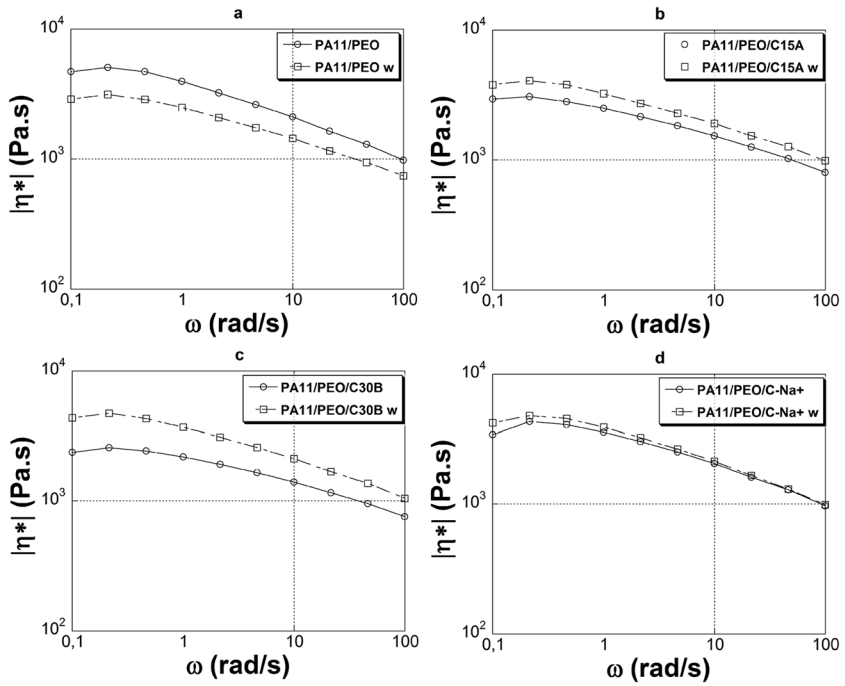

Fig. 9 Comparison of water-assisted to dry-processed complex viscosity $|\eta^*|$ as a function of the frequency ω of (a) the unfilled PA11/PEO, and blends containing (b) C15A, (c) C30B and (d) C-Na^+.

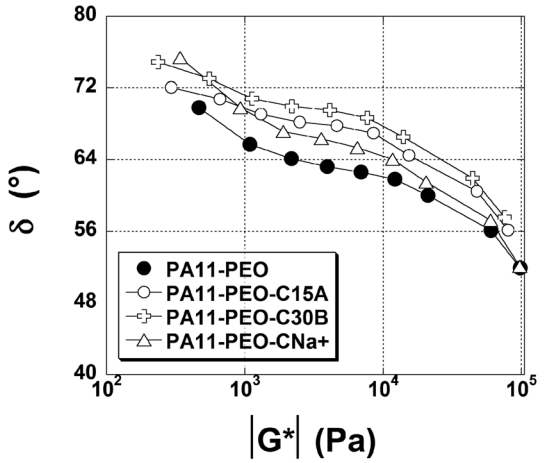

Fig. 10 van Gurp–Palmen plot (phase angle, δ, *versus* absolute complex modulus, $|G^*|$) of the unfilled and clay-based PA11/PEO.

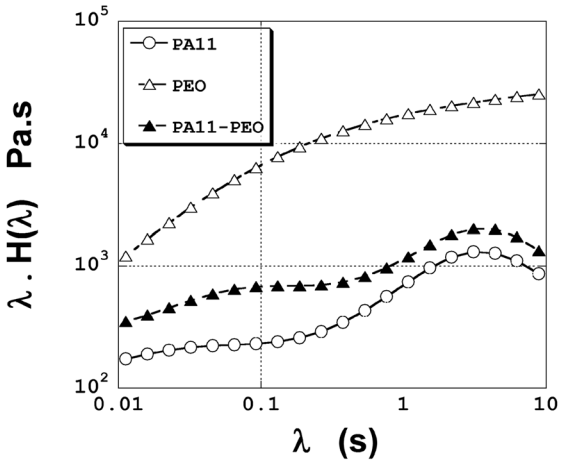

Fig. 12 Weighted relaxation spectra of PA11, PEO and PA11/PEO blend.

with a shoulder at about 0.7 s. This observation may be ascribed to a catalytic action of C-Na^+ on the pyrolysis of PA11 and PEO due to the presence of Si–OH and Al–OH acid sites on the external surface of the clay. Such catalytic effect of C-Na^+ has already been discussed in the literature for the thermal degradation of different polymers.[53,62,63] According to the authors, C-Na^+ presents Brønsted acid sites such as Si–OH and Al–OH on the external surface of clay which promote the polymer degradation. With random chain scissions, a broadening of the distribution of the relaxation spectrum is the consequence. The broadening of the PA11 and PEO characteristic relaxation time obtained in the presence of the organoclay (C15A and C30B) and the slight shift of the maxima of PA11 towards a lower relaxation time indicate an increase in the polydispersity of the chains relaxations.

Fig. 14 shows the effect of the water-assisted extrusion process on the weighted relaxation spectra of the different blends. The $\lambda H(\lambda)$ plot of PA11/PEO blend processed by the water-assisted extrusion is lower due to the hydrolysis of PEO. The shoulder of PEO was flattened indicating the effect of water

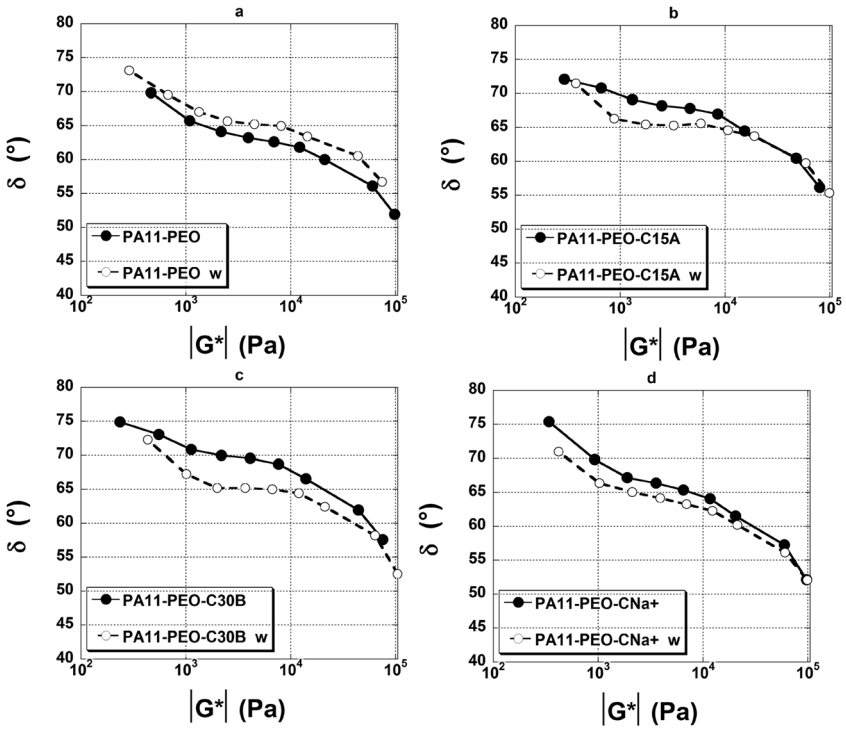

Fig. 11 van Gurp–Palmen plot (phase angle, δ, *versus* absolute complex modulus, $|G^*|$) of the blends prepared without and with water. Unfilled (a) PA11/PEO, blend containing (b) C15A, (c) C30B and (d) C-Na^+.

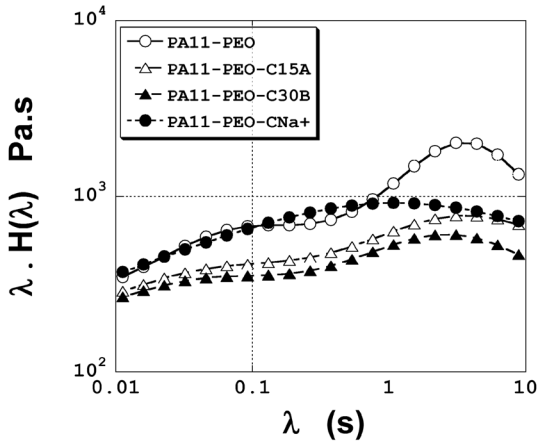

Fig. 13 Weighted relaxation spectra of unfilled and clay-based PA11/PEO blends.

on the relaxation distribution of PEO, and the PA11 peak was shifted towards the lower relaxation times illustrating a slight compatibilizing effect. This behaviour is consistent with the previous vGP analysis.

In the case of C15A filled composite, the increase in the height of the maxima corresponding to the PA11 matrix prepared by water-assisted extrusion reflects an additional relaxation of chains in the vicinity of the clay polymer interface due to its better dispersion mainly localized in the PA phase.[61] In the case of PA11/PEO/C30B blend, the shoulder corresponding to the PEO phase was additionally more affected by the water-assisted extrusion probably because of the localization of more organoclay particles into the PEO which leads to the enhanced elasticity.[64] Moreover the PA11 sharp peak is due to the well dispersed clay platelets into the polymer matrix as previously shown by TEM. The behaviour of the C-Na^+ blend is dramatically changed with the water-assisted extrusion. In absence of water, the shape of the relaxation of the materials consists of a single large peak. With the addition of water, the relaxation peaks of PA11 and PEO both reappear. It is explained by the presence of water limiting the degradation of polymer induced by nanofiller. Similar behaviour was observed by Stoclet *et al.* in the case of NaMMT/PA11 and HNT/PLA composites.[63,65] The authors stipulate that in the case of the compounds elaborated with water injection, the adsorption of water to the surface of the montmorillonite prevents the initiation of degradation of polymers by adsorbing water onto the clay surface and forming phase separation from polymer. In addition, the lubricant effect of water may decrease the local shear force and thus prevents mechanoscissions of polymer chains.[66]

Thermogravimetric analysis (TGA)

Since the rheological results showed that the blends were more or less affected by degradation depending on processing conditions, the thermal stability of different blends was then evaluated by TGA. The weight evolution as function of the temperature is presented in Fig. 15, and the values of the onset of decomposition temperature corresponding to 5% weight loss, the maximum degradation temperature and the residue content are summarized in Table 2. As it can be seen, PA11 exhibits a much higher thermal stability than PEO. The blend

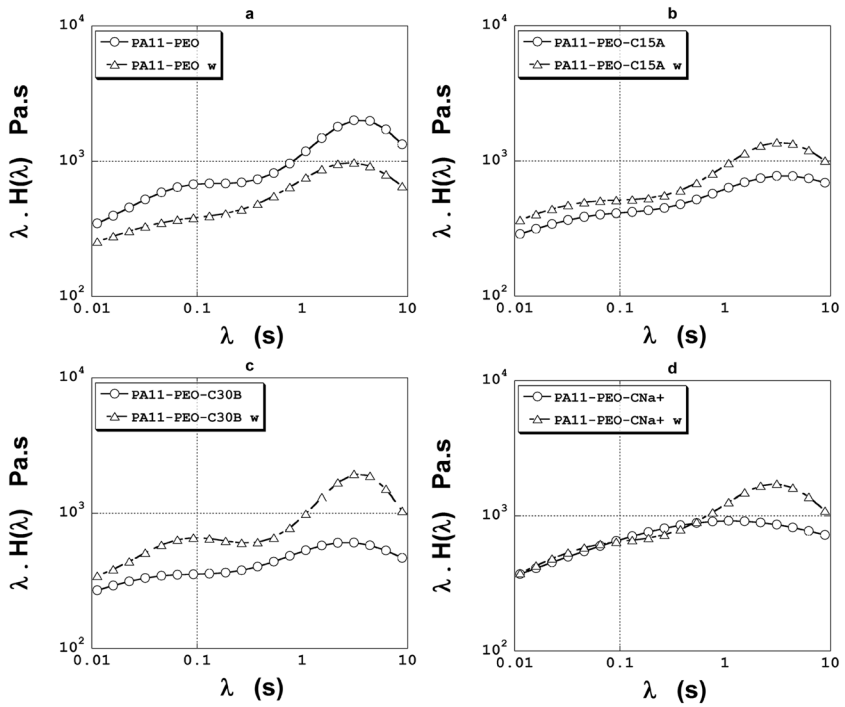

Fig. 14 Weighted relaxation spectra of the blends prepared without and with water-assisted extrusion. Unfilled blend (a) PA11/PEO, blend containing (b) C15A, (c) C30B and (d) C-Na^+.

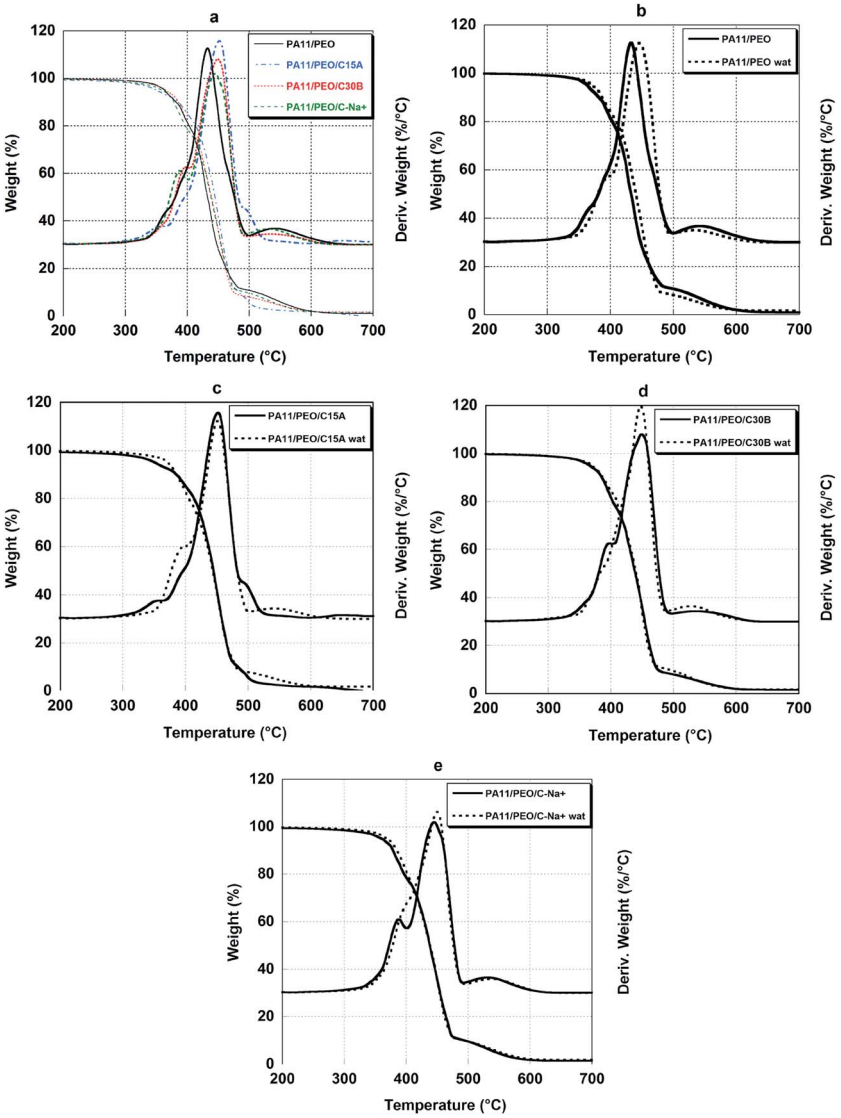

Fig. 15 Weight loss percentage and derivative as a function of temperature of unfilled and clay-filled PA11/PEO blends, (a) without and (b–e) with injection of water.

showed a thermal stability closer to that of PA11. In the PA11/PEO blend, only the degradation peak of PA11 can be observed, probably due to the low content of PEO. With the addition of clay no significant changes are observed for the onset of degradation due to the very low amount of clay. Similar results have been reported for the PA6 nanocomposites, under air 5 wt% clay addition increasing the onset temperature by only ~3 °C.[67] Concerning the maximum degradation temperature, it is increased by ~15 °C for all blends with clay compared to the unfilled blend. The improvement of thermal stability could be explained by the barrier effect of clay layers to in-diffusion of oxygen and to the out-diffusion even trapped of degraded small molecules.[13,68] The slight decrease of degradation onset at 5 wt% is probably due to the clay-catalyzed degradation of polymers.[13,14,69]

When water is injected, both the onset and the maximum of degradation show that thermal stabilities of the unfilled blend and clay-based blends are slightly improved. It has already been reported that water could limit the degradation of polyamide.[53,70] In case of clay-based blends, water brings about higher exfoliation level of clay with increased barrier effect. Moreover, the catalytic effect of clay on polymer degradation is softened with the aid of water, increasing thus the overall thermal stability of blends. The improved thermal stability of the unfilled and clay-based blends is also confirmed by the increased content of residue after injection of water.

Conclusion

In this study we have prepared PA11/PEO/clay ternary mixtures using both unmodified (Cloisite Na^+) and organomodified clays (Cloisite 15A and C30B) to evaluate the effect of clay on PA11/PEO blend. In addition to the normal dry-processed extrusion,

Table 2 Onset and maximum of thermal degradation and residue content

	$T_{5\ wt\%}$ (°C)	T_{max} (°C)	Residue (%)
PA11	389	424	0.25
PEO	226	267	2.08
PA11/PEO 80/20	369	433	1.00
PA11/PEO 80/20 w	376	447	1.69
1% C-Na^+	365	445	1.44
1% C-Na^+ w	374	450	1.94
1% C15A	357	452	1.52
1% C15A w	377	451	1.72
1% C30B	371	449	1.59
1% C30B w	375	458	1.70

the water-assisted process was used to highlight the effect of water on the properties of different blends.

The miscibility of PA11 or PEO with water in the extrusion conditions was evidenced by HPDSC tests, inducing the cryoscopic effect. TEM observations showed that clay platelets were almost selectively localized in the PA11 matrix phase. With the injection of water during extrusion, some clay platelets were localized in the PEO dispersed phase instead of the PA11 matrix in the case of Cloisite 15A and C30B. In the case of Cloisite Na^+, clay platelets stayed in PA11 even if water was injected during extrusion.

Rheological tests showed that water-assisted process increased both the modulus and viscosity of nanocomposites due to a better dispersion state. The van Gurp–Palmen plot also indicated a decreased interfacial tension between PA11 and PEO responsible for the reduced size of the dispersed phase when clay of any kind is added. On the other hand the weighted relaxation spectra confirmed the catalytic effect of Cloisite Na^+ on the degradation of polymers, while this effect was deleted in presence of water.

As showed by TGA, the presence of clay improved the thermal stability of the unfilled PA11/PEO blend due to the barrier effect of clay, limiting the degradation. With the injection of water, thermal stability of all blends was increased as a result of better dispersion state.

The results of our work reveal that water-assisted extrusion is a very promising processing method as it can be used to improve the dispersion state of clay, and tune the localization of clay in an immiscible polymer blend. The thermal stability and rheological properties could be enhanced thanks to the limited degradation of polymers in the presence of water.

Acknowledgements

This work was supported by International Campus on Safety and Intermodality in Transportation (CISIT), Nord-Pas-de-Calais Region and European Community (FEDER).

References

1 *Polymer Blends*, ed. D. R. Paul and C. B. Bucknall, Wiley, New York, 2000, vol. 1, pp. 539–580.
2 *Polymer Blends Handbook*, ed. L. A. Utracki, Kluwer Academic, Dordrecht, 2002, vol. 1, pp. 352–387.
3 B. Gupta, M. F. Lacrampe and P. Krawczak, *Polym. Polym. Compos.*, 2006, **14**, 13–38.
4 K. Renner, S. Henning, J. Moczo, M. S. Yang, H. J. Choi and B. Pukanszky, *Polym. Eng. Sci.*, 2007, **47**, 1235–1245.
5 M. Kontopoulou, Y. Liu, J. R. Austin and J. S. Parent, *Polymer*, 2007, **48**, 4520–4528.
6 J. S. Hong, H. Namkung, K. H. Ahn, S. J. Lee and C. Kim, *Polymer*, 2006, **47**, 3967–3975.
7 B. B. Khatua, D. J. Lee, H. Y. Kim and J. K. Kim, *Macromolecules*, 2004, **37**, 2454–2459.
8 M. Si, T. Araki, H. Ade, A. L. D. Kilcoyne, R. Fisher, J. C. Sokolov and M. H. Rafailovich, *Macromolecules*, 2006, **39**, 4793–4801.
9 R. A. Vaia, R. K. Teukolsky and E. P. Giannelis, *Chem. Mater.*, 1994, **6**, 1017–1022.
10 A. Okada and A. Usuki, *Macromol. Mater. Eng.*, 2006, **291**, 1449–1476.
11 O. Monticelli, Z. Musina, A. Frache, F. Bellucci, G. Camino and S. Russo, *Polym. Degrad. Stab.*, 2007, **92**, 370–378.
12 T. D. Fornes, P. J. Yoon and D. R. Paul, *Polymer*, 2003, **44**, 7545–7556.
13 A. Leszczynska, J. Njuguna, K. Pielichowski and J. R. Banerjee, *Thermochim. Acta*, 2007, **453**, 75–96.
14 W. Xie, Z. M. Gao, W. P. Pan, D. Hunter, A. Singh and R. Vaia, *Chem. Mater.*, 2001, **13**, 2979–2990.
15 J. M. Cervantes-Uc, J. V. Cauich-Rodriguez, H. Vazquez-Torres, L. F. Garfias-Mesias and D. R. Paul, *Thermochim. Acta*, 2007, **457**, 92–102.
16 T. X. Liu, K. P. Lim, W. C. Tjiu, K. P. Pramoda and Z. K. Chen, *Polymer*, 2003, **44**, 3529–3535.
17 R. A. Korbee and A. A. Van Geenen, *US Pat.*, 6 350 805, 1997.
18 N. Fedullo, M. Sclavons, C. Bailly, J. M. Lefebvre and J. Devaux, *Macromol. Symp.*, 2006, **233**, 235–245.
19 Z. Z. Yu, H. U. Guo-Hua, J. Varlet, A. Dasari and Y. W. Ma, *J. Polym. Sci., Part B: Polym. Phys.*, 2005, **43**, 1100–1112.
20 B. Bhandari, B. D'Arcy and G. Young, *Int. J. Food Sci. Technol.*, 2001, **36**, 453–461.
21 C. Thouzeau, C. Henneuse, M. Sclavons, J. Devaux, J. Soulestin and G. Stoclet, *Polym. Degrad. Stab.*, 2013, **98**, 557–565.
22 *Polymer Data Handbook*, ed. J. E. Mark, Oxford University Press, New York, 1999, p. 542.
23 J. S. Shelley, P. T. Mather and K. L. DeVries, *Polymer*, 2001, **42**, 5849–5858.
24 P. C. Yuang and Y. H. Shen, *J. Colloid Interface Sci.*, 2005, **285**, 443–447.
25 S. Mathur and B. M. Moudgil, *J. Colloid Interface Sci.*, 1997, **196**, 92–98.
26 C.-C. Su and Y.-H. Shen, *J. Colloid Interface Sci.*, 2009, **332**, 11–15.
27 *Particle Size Measurements: Fundamentals, Practice, Quality*, ed. H. G. Merkus, Springer, Dordrecht, 2009, p. 15.
28 S. Prodduturi, R. V. Manek, W. M. Kolling, S. P. Stodghill and M. A. Repka, *J. Pharm. Sci.*, 2005, **94**, 2232–2245.

29 I. McDougall, N. Orbey and J. M. Dealy, *J. Rheol.*, 2014, **58**, 779–797.
30 M. G. M. Wevers, T. F. J. Pijpers and V. B. F. Mathot, *Thermochim. Acta*, 2007, **453**, 67–71.
31 K. Charlet, V. Mathot and J. Devaux, *Polym. Int.*, 2011, **60**, 119–125.
32 W. Wagner, J. R. Cooper, A. Dittmann, J. Kijima, H. J. Kretzschmar, A. Kruse, R. Mares, K. Oguchi, H. Sato, I. Stocker, O. Sifner, Y. Takaishi, I. Tanishita, J. Trubenbach and T. Willkommen, *J. Eng. Gas Turbines Power*, 2000, **122**, 150–182.
33 A. Seeger, D. Freitag, F. Freidel and G. Luft, *Thermochim. Acta*, 2004, **424**, 175–181.
34 S. Gogolewski and A. J. Pennings, *Polymer*, 1975, **16**, 673–679.
35 S. Rastogi, A. E. Terry and E. Vinken, *Macromolecules*, 2004, **37**, 8825–8828.
36 D. F. Wu, C. X. Zhou, X. Fan, D. L. Mao and Z. Bian, *Polym. Degrad. Stab.*, 2005, **87**, 511–519.
37 R. Puffr and J. Sebenda, *J. Polym. Sci., Part C: Polym. Symp.*, 1967, **16**, 79–93.
38 J. Derho, J. Soulestin and P. Krawczak, *J. Appl. Polym. Sci.*, 2014, **131**, 40426.
39 L. Elias, F. Fenouillot, J. C. Majeste, G. Martin and P. Cassagnau, *J. Polym. Sci., Part B: Polym. Phys.*, 2008, **46**, 1976–1983.
40 J. Y. Feng, C. M. Chan and J. X. Li, *Polym. Eng. Sci.*, 2003, **43**, 1058–1063.
41 P. K. S. Mural, G. Madras and S. Bose, *RSC Adv.*, 2014, **4**, 4943–4954.
42 K. E. Strawhecker and E. Manias, *Chem. Mater.*, 2003, **15**, 844–849.
43 M. Fermeglia, M. Ferrone and S. Pricl, *Fluid Phase Equilib.*, 2003, **212**, 315–329.
44 G. Tanaka and L. A. Goettler, *Polymer*, 2002, **43**, 541–553.
45 J. Rubio and J. A. Kitchener, *J. Colloid Interface Sci.*, 1976, **57**, 132–142.
46 J. Reignier, B. D. Favis and M. C. Heuzey, *Polymer*, 2003, **44**, 49–59.
47 G. Serpe, J. Jarrin and F. Dawans, *Polym. Eng. Sci.*, 1990, **30**, 553–565.
48 W. Lerdwijitjarud, A. Sirivat and R. G. Larson, *Polym. Eng. Sci.*, 2002, **42**, 798–809.
49 T. D. Fornes, P. J. Yoon and D. R. Paul, *Abstracts of Papers of the American Chemical Society*, 2002, vol. 224, pp. U493–U493.
50 T. D. Fornes, P. J. Yoon, H. Keskkula and D. R. Paul, *Polymer*, 2001, **42**, 9929–9940.
51 G. Galgali, C. Ramesh and A. Lele, *Macromolecules*, 2001, **34**, 852–858.
52 *Polymer-Clay Nanocomposites*, ed. T. J. Pinnavaia and G. W. Beall, Wiley, New York, 2000, p. 315.
53 F. Touchaleaume, J. Soulestin, M. Sclavons, J. Devaux, M. F. Lacrampe and P. Krawczak, *Polym. Degrad. Stab.*, 2011, **96**, 1890–1900.
54 S. Trinkle, P. Walter and C. Friedrich, *Rheol. Acta*, 2002, **41**, 103–113.
55 K. Prashantha, J. Soulestin, M. F. Lacrampe, P. Krawczak, G. Dupin and M. Claes, *Compos. Sci. Technol.*, 2009, **69**, 1756–1763.
56 M. Abdel-Goad, P. Poetschke, D. Zhou, J. E. Mark and G. Heinrich, *J. Macromol. Sci., Part A: Pure Appl.Chem.*, 2007, **44**, 591–598.
57 C. Carrot, S. Mbarek, M. Jaziri, Y. Chalamet, C. Raveyre and F. Prochazka, *Macromol. Mater. Eng.*, 2007, **292**, 693–706.
58 R. M. Li, W. Yu and C. X. Zhou, *Polym. Bull.*, 2006, **56**, 455–466.
59 M. R. Nobile and F. Cocchini, *Rheol. Acta*, 2008, **47**, 509–519.
60 J. Honerkamp and J. Weese, *Macromolecules*, 1989, **22**, 4372–4377.
61 R. Al-Itry, K. Lamnawar and A. Maazouz, *Rheol. Acta*, 2014, **53**, 501–517.
62 Q. Zhou and M. Xanthos, *Polym. Degrad. Stab.*, 2009, **94**, 327–338.
63 G. Stoclet, M. Sclavons, B. Lecouvet, J. Devaux, P. van Velthem, A. Boborodea, S. Bourbigot and N. Sallem-Idrissi, *RSC Adv.*, 2014, **4**, 57553–57563.
64 G. Basseri, M. M. Mazidi, F. Hosseini and M. K. R. Aghjeh, *Polym. Bull.*, 2014, **71**, 465–486.
65 G. Stoclet, M. Sclavons and J. Devaux, *J. Appl. Polym. Sci.*, 2013, **127**, 4809–4824.
66 S. J. de Jong, E. R. Arias, D. T. S. Rijkers, C. F. van Nostrum, J. J. Kettenes-van den Bosch and W. E. Hennink, *Polymer*, 2001, **42**, 2795–2802.
67 K. P. Pramoda, T. X. Liu, Z. H. Liu, C. B. He and H. J. Sue, *Polym. Degrad. Stab.*, 2003, **81**, 47–56.
68 M. Tarameshlou, S. H. Jafari, H. A. Khonakdar, M. Farmahini-Farahani and S. Ahmadian, *Polym. Compos.*, 2007, **28**, 733–738.
69 H. L. Qin, S. M. Zhang, C. G. Zhao, M. Feng, M. S. Yang, Z. J. Shu and S. S. Yang, *Polym. Degrad. Stab.*, 2004, **85**, 807–813.
70 F. Touchaleaume, J. Soulestin, M. Sclavons, J. Devaux, F. Cordenier, P. van Velthem, J. J. Flat, M. F. Lacrampe and P. Krawczak, *eXPRESS Polym. Lett.*, 2011, **5**, 1085–1101.

